THE APPLICATION OF THE GENETIC ALGORITHM-BACK PROPAGATION NEURAL NETWORK ALGORITHM IN THE HIGH-ENERGY PHYSICS

[1]M.Y. El-Bakry, [2,3]E.A. El-Dahshan, [3]A. Radi, [1]M. Tantawy, [1,4]M.A. Moussa

[1]*Ain Shams University, Faculty of Education, Physics Department, Roxi, Cairo, Egypt*
[2]*Egyptian E-Learning University- 33 El-mesah St., El-Dokki- Giza- Postal code 11566*
e-mail: seldahshan@eelu.edu.eg
[3]*Ain Shams University, Faculty of Sciences, Physics Department, Abbassia, Cairo, Egypt*
[4]*Buraydah Colleges, Al-Qassim, Buraydah, King Abdulazziz Road, East Qassim University, P.O.Box 31717, KSA*
e-mail: moaaz2030@yahoo.com
Received April 18, 2016

Multiparticle production mechanism is one of the most phenomena that the high-energy physics concerns. In this work, the evolutionary genetic algorithm (GA) is used to optimize the parameters of the back-propagation neural networks (BPNN). The hybrid evolutionary-neuro model (GA-BPNN) was trained to simulate the rapidity distribution $\left(\frac{1}{N}\frac{dN}{dY}\right)$ of positive and negative pions for $\overline{p}-Au, \overline{p}-Ag \text{ and } \overline{p}-Mg$ interactions at lab momentum (P_{Lab}) =100 GeV/c. Also, for total charged, positive and negative pions for $\overline{p}-Ar, \overline{p}-Xe$ interactions at P_{Lab}= 200 GeV/c. Finally, total charged particles for $p-Pb$ collision at center-of-mass energy $\left(\sqrt{s}\right)$ = 5.02 TeV are simulated. An efficient ANN network with different connection parameters (weights and biases) have been designed by the GA to calculate and predict the rapidity distribution as a function of the lab momentum (P_{Lab}), mass number (A) and the number of particles per unit solid angle (Y). Our simulated results have been compared with the experimental data and the matching has been clearly found. It is indicated that the developed GA-BPNN model for rapidity distribution was more successful.
KEY WORDS: High and ultrahigh energy physics, hadron-nucleus (h-A) interactions, rapidity distribution, modeling and simulation, hybrid evolutionary-neuro model

ЗАСТОСУВАННЯ ГЕНЕТИЧНОГО АЛГОРИТМУ–АЛГОРИТМУ НЕЙРОННОЇ МЕРЕЖІ ЗІ ЗВОРОТНИМ ЗВ'ЯЗКОМ У ФІЗИЦІ ВИСОКИХ ЕНЕРГІЙ

Механізм створення багаточасткових пучків є одним із великого ряду явищ, пов'язаних з фізикою високих енергій. У цій роботі використовується еволюційний генетичний алгоритм (GA), для оптиміззації параметрів нейронних мереж із зворотним зв'язком (BPNN). Гібридна еволюційна нейромодель (GA - BPNN) була підготовлена для моделювання розподілу швидкості $\left(\frac{1}{N}\frac{dN}{dY}\right)$ потоків позитивних і негативних піонів достатніх для взаємодії $\overline{p}-Au, \overline{p}-Ag \text{ and } \overline{p}-Mg$, при імпульсі в лабораторній системі (P_{Lab}) =100 GeV/c, а також для усього об'єму заряджених позитивних і негативних піонів для взаємодій $\overline{p}-Ar, \overline{p}-Xe$ при P_{Lab} = 200 GeV/c. I, нарешті, моделюється повний об'єм заряджених часток для зіткнення $p-Pb$ при енергії в системі центра мас $\left(\sqrt{s}\right)$ = 5.02 TeV. За допомогою GA розроблена ефективна мережа ANN з різними параметрами зв'язку (вага і зміщення), щоб вичислити і передбачити розподіл швидкостей як функцію експериментального імпульсу, масового числа (A) і кількості часток на тілесний кут (Y). Будо проведено порівняня результатів нашого моделювання з експериментальними даними, і була визначена їх відповідність один одному. Відмічено, що модернізована модель GA - BPNN для розподілу швидкості дає вищі результати.
КЛЮЧОВІ СЛОВА: фізика високих і надвисоких енергій, адронно-ядерні (h - A) взаємодії, розподіл швидкостей, розрахунок і моделювання, гібридна еволюційна нейромодель

ПРИМЕНЕНИЕ ГЕНЕТИЧЕСКОГО АЛГОРИТМА – АЛГОРИТМА НЕЙРОННОЙ СЕТИ С ОБРАТНОЙ СВЯЗЬЮ В ФИЗИКЕ ВЫСОКИХ ЭНЕРГИЙ

Механизм создания многочастичных пучков является одним из большого ряда явлений, связанных с физикой высоких энергий. В этой работе используется эволюционный генетический алгоритм (GA) для оптимизации параметров нейронных сетей с обратной связью (BPNN). Гибридная эволюционная нейромодель (GA-BPNN) была подготовлена для моделирования распределения скорости $\left(\frac{1}{N}\frac{dN}{dY}\right)$ потоков положительных и отрицательных пионов достаточных для взаимодействия $\overline{p}-Au, \overline{p}-Ag \text{ and } \overline{p}-Mg$ при импульсе в лабораторной системе (P_{Lab}) =100 ГэВ/c, а также для всего объема заряженных положительных и отрицательных пионов для взаимодействий $\overline{p}-Ar, \overline{p}-Xe$ при P_{Lab} = 200 ГэВ/c. И, наконец, моделируется полный объем заряженных частиц для столкновения $p-Pb$ при энергии в системе центра масс $\left(\sqrt{s}\right)$ = 5.02 ТэВ. С помощью GA разработана эффективная сеть ANN с различными параметрами связи (вес и смещение), для вычисления и предсказания распределения скоростей как функции экспериментального импульса (P_{Lab}) и количества частиц на телесный угол (Y). Проведено сравнение результатов нашего моделирования с экспериментальными

данными, и было определено их соответствие друг другу. Отмечено, что модернизированная модель GA-BPNN для распределения скорости дает более высокие результаты.

КЛЮЧЕВЫЕ СЛОВА: физика высоких и сверхвысоких энергий, адронно-ядерные (h-A) взаимодействия, распределение скоростей, расчет и моделирование, гибридная эволюционная нейромодель

Rapidity distribution of hadron-nucleus (h-A) interactions have been studied as one example of the parameters controlling multiparticle production mechanism in high and ultrahigh energy physics. Many models studied the hadron structure [1-5] and the interactions between hadrons and nuclei such as fragmentation model [6-8], quark model [9-11], the three-fireball model [12] and many more.

Our group [13-16] studied the applications of artificial intelligence and the evolutionary computation techniques such as neural network, adaptive fuzzy inference system, genetic programming, genetic algorithm, hybrid technique model and many others to solve many complex (nonlinear) problems in high-energy physics and showed best fitting with the corresponding experimental data in comparison with the conventional techniques.

With the emergence of the computer simulation technology, it greatly reduces the time, space and cost. Therefore, the computer simulation technology has become a powerful tool for the research of the high-energy physics and its development will have a positive reference and guiding role for the experimental physicists. We used the hybrid Genetic Algorithm (GA) and Back-propagation Neural Network (BPNN) technique (GA-BPNN) [15] as a tool to discover the equations that govern some sub-nuclear interactions at high and ultrahigh energies. Based on this idea, according to the real data of the rapidity distribution for hadron-nucleus (h-A) collisions taken in ALICE (2013) and in many other labs, this paper focused on the rapidity distribution $\left(\frac{1}{N}\frac{dN}{dY}\right)$ of positive and negative pions for (antiproton ($\bar{p}$) –nucleus (A)) $\bar{p} - Au, \bar{p} - Ag$ and $\bar{p} - Mg$ interactions at Lab Momentum (P_{Lab}) =100 GeV/c [17], total charged, positive and negative pions for $\bar{p} - Ar, \bar{p} - Xe$ interactions at $P_{Lab} = 200$ GeV/c [18-20] and total charged particles for (proton (P) –nucleus (A)) $p - Pb$ collision at center-of mass energy $\left(\sqrt{s}\right)$ = 5.02 TeV [21]. In addition, it established intelligent prediction model by means of smart algorithm. Through the constant optimization of the algorithms and models, it achieved more accurate prediction of unknown data for rapidity distribution.

The research of this topic has a certain reference value for experimental high-energy physicists, and has a positive guiding significance in the field of high-energy physics.

In this article, hybrid model has been used to discover a function that computes the rapidity distribution $\left(\frac{1}{N}\frac{dN}{dY}\right)$ of positive and negative pions for $\bar{p}$-Au, $\bar{p}$-Ag and $\bar{p}$-Mg interactions at 100 GeV/c [17], the rapidity distribution of created (total charged, positive and negative) pions for $\bar{p} - Ar, \bar{p} - Xe$ collisions at P_{Lab} =200 GeV/c [18-20] and the rapidity distribution of total charged particles for $p - Pb$ collision at $\left(\sqrt{s}\right)$ = 5.02 TeV [21]. The discovered functions produced by the hybrid model show an excellent matching when they have been compared to the corresponding experimental data [18-21]. This article is organized as follows; Section **PREDICTION MODEL OF RAPIDITY DISTRIBUTION FOR (h-A) COLLISIONS BASED ON BPNN ALGORITHM** gives the outlines to the basics of the BP Algorithm. Section **SIMULATION MODELING** reviews the Genetic Algorithm and Back-Propagation Neural Network models and how to be implemented. Modeling of the rapidity distribution using GA-BPNN is provided in Section **MODEL OF GA-BP OF THE RAPIDITY DISTRIBUTION FOR (h-A) COLLISIONS**. Section **RESULTS AND DISCUSSIONS** shows the simulation results and discussion. Finally, conclusions are provided in Section **CONCLUSIONS**.

PREDICTION MODEL OF RAPIDITY DISTRIBUTION FOR (h-A) COLLISIONS BASED ON BPNN ALGORITHM

We have performed the modeling of the inclusive interaction

$$\bar{p} - Au, \bar{p} - Ag, \bar{p} - Mg \rightarrow \pi^{\pm} + X \qquad (1)$$

at momentum of antiprotons 100 GeV/c [18]. This experiment was performed with the Fermi lab 30-inch bubble chamber and downstream Particles Identifier to study inclusive charged pion production in the high-energy interactions of $\bar{p}$ with thin foils of magnesium, silver and gold. All data are similar and display the following features. We observe that in the backward direction [18] they rise rapidly with increasing A. As the rapidity increases, the A dependence becomes weaker and in the region y ≈ 4.5 the distributions become almost independent of A. We also do not observe any region where a rapidity plateau exists.

Experimental data on antiproton-nucleus ($\bar{p} - A$) collisions [18-20] at momentum of antiprotons 200 GeV/c were performed to study inclusive total charged, positive and negative pion production in the high-energy interactions of $\bar{p}$ with thin foils of Argon and Xenon.

The pions rapidity distribution of shower and negative particles for $\bar{p} - Xe$ and $\bar{p} - Ar$ in center-of-mass system

(CMS) is shifted by 3 units, when the projectile incident momentum is $P_{Lab} = 200$ GeV/c, from the laboratory system using Eq. (2).

$$y^{/} = y + \frac{1}{2}\ln\left(\frac{1-\beta}{1+\beta}\right), \tag{2}$$

where, $y^{/}$ CMS rapidity, β is CMS velocity and y is lab system rapidity which is defined as [22-24],

$$y = \frac{1}{2}\ln\left(\frac{E + P_{//}}{E - P_{//}}\right) = \sinh^{-1}\left(\frac{P_{//}}{\mu}\right) \tag{3}$$

E and $P_{//}$ are the total energy and longitudinal momentum of particle (C) produced in the inclusive process (hadron-nucleus),

$$h + A = C + X \qquad \text{(X means any other particle or particles)}$$

Where, h is any hadron, A is the nucleus.
The quantity μ is the transverse mass of the pion, which is defined as,

$$\mu = (m_{\circ}^{2} + p_{t}^{2})^{1/2}, \tag{4}$$

where, m_{o} is the rest mass of the pion and p_{t} is its transverse momentum

p − Pb collisions [21] at center-of-mass energies of $\sqrt{s} = 5.02$ .TeV have recently been performed at the LHC. The rapidity dependence is somewhat flat and slightly steeper in the higher energy p − Pb collisions.

The GA-BPNN Algorithm has been used to determine gradually the optimal number of neurons in the hidden layers of neural network as well as simulate and predict eventually the rapidity distribution for (h-A) collisions at $P_{Lab} = 100, 200$ GeV/c and $\sqrt{s} = 5.02$ TeV.

We recorded that the BP network needs the evolution generations to meet preset accuracy requirements in the different numbers of units in hidden layer. Moreover, after the evolution of each network was completed, we input test data to verify its accuracy and calculated the respective prediction error of average. After the network structure was determined, we input training data for network training, saved network structure after training, and input forecasting data validation. In addition, we analyzed the prediction error between the actual output data and the desired ones, thus evaluating the performance of BP network prediction of the rapidity distribution for (h-A) collisions at $P_{Lab} = 100$, 200 GeV/c and $\sqrt{s} = 5.02$ TeV.

The BP neural network can achieve the detection of the rapidity distribution for (h-A) collisions at 100, 200 GeV/c and 5.02 TeV, but the accuracy and speed need to further improve. BP algorithm only adjusted connection weights of neural network from the local angle but did not examine the whole learning process form the global perspective. Therefore, it is easy to converge to local minimum.

SIMULATION MODELING
Artificial neural network

ANNs are simple mathematical models of nervous systems and adaptive biological learning [25]. These soft data based computational methods can model multidimensional non-linear processes and represent complex input–output relation. ANNs are one of the best candidates for experimental data modeling, function approximation and on-line data processing.

ANNs structure consists of a set of processing units, normally arranged in layers, known as neurons. These neurons interact with weighted connection known as synaptic weights. A neuron performs certain computation called activation function:

$$f(x) = \frac{e^{x} - e^{-x}}{e^{x} + e^{-x}} \tag{5}$$

exerted on sum of weighted inputs of the neuron (x), as indicated in the below equation

$$O = f\left(b + \sum_{i} w_{i} p_{i}\right), \tag{6}$$

where O is the neuron output, f the activation (transfer) function, b the bias, w_{i} the neuron weight and p the neuron input. Weights can be determined adaptively by learning algorithm and can store the acquired knowledge. The learning algorithm adjusts weights to handle given problems. In most cases, the ANNs are trained by a set of input–output data. This training process is known as supervised learning [25].

The number of neurons in input and output layers is the same as the number of inputs and outputs of the problem, respectively. Number of hidden layers (between input layer and output layer) and number of their neurons are free

parameters and usually can be determined and optimized by trial and error. Multi Layer Perceptrons (MLPs) are extensively applied to feed forward ANNs that need supervised learning. Usually, training and testing data shall be normalized to increase the performance of network. A MLP with one or more hidden layers can approximate any non-linear mapping to any accuracy degree [25].

Genetic algorithm

The Genetic Algorithm is a type of evolutionary computation [26]. It mimics two mechanisms of natural selection and evolution of biological species [26]. This iterative probabilistic searching method is used in complex multi-dimensional optimization problems resulting in a fittest solution. The GA is based on a constant-size population of chromosomes which can be expressed as a string of bits, 0 or 1 s, corresponding to a possible solution to the problem. A chromosome includes some segments, each of them corresponding to encoding of problem variables. An initial population is randomly produced. In this population, the fitness function of each chromosome is evaluated. Next, certain numbers of them are selected as parents for reproduction [26]. Fitter chromosomes have more chance to be selected. Each pair of chromosomes is randomly selected and merged by crossover operator and offspring produced thereby. One or more bits of a random selected chromosome of offspring are altered by a mutation operator. Mutation enables the optimization to get out of local optima trap and to find global optima. Offspring and some of parents provide subsequent population. The evolution cycle is continued until algorithm converges to the best chromosome which represents the optimal solution [26]. We used Mean Squared Error (MSE) as a tool to calculate the performance of the selected topology to the considered output (rapidity distribution).

The difference between the real rapidity distribution and estimated rapidity distribution can be represented by Mean Squared Error (MSE) standard:

$$\text{MSE} = \frac{1}{N} \sum_{i=1}^{N} (x_1(i) - x_2(i))^2,$$ (7)

where $x_1(i)$ and $x_2(i)$ are the values of real and calculated rapidity distribution in time domain and N is number of sample points.

MODEL OF GA-BPNN OF THE RAPIDITY DISTRIBUTION FOR (h-A) COLLISIONS

Genetic algorithm does not use external information in the process of the evolutionary search and is only based on the fitness function. Therefore, it is crucial for choosing fitness function, which directly affects the convergence rate of genetic algorithm and the ability to find the optimal solution. Since the objective function is error sum of squares of the neural network, and for getting its minimum value, so the fitness function adapts the inverse of error function. The selecting operation used fitness proportion, which is the most common way, the cross-used the method of arithmetic crossover, and variation method used the operation of non-uniform mutation.

If the value of the fitness function, the optimal individual corresponding to, met accuracy requirements or reached iterations that we set, or the range of the average fitness value changed lastly that was less than a certain constant and over a certain algebra, then we finished the training. At this time, we set the individual that had the largest fitness as output of the optimal solution, and it was the initial weight and threshold that need to be optimized. Otherwise, we continued the cycle. After reordering the current parent and offspring, we chose N individuals that had higher fitness value as the next generation of the group. In addition, we computed its fitness and trained them again until satisfying the termination conditions of the above.

We decoded the optimal solution, which was obtained from genetic algorithm, and we assigned them to BP network without starting training as initial weights of BP network. Then, according to BP algorithm, we input training samples for training and learning of the network and calculated the error between the output value and the expected value. If it was beyond the precision requirement, then we turned to the back propagation process and returned the error signal along the way. At the same time, according to the size of the error of each layer, we adjusted its weights and thresholds layer and layer. Until the error was less than given value $5.98\,e^{-04}$, or it reached the training number predetermined, then we ended BP algorithm. We saved the weight and the threshold of hidden layer that had been trained as the new initial weights and the threshold of the network and then input the test sample for simulation.

The setting of BP algorithm parameters was as follows: the rate of the initial learning was 0.08, number of epochs = 2000, the transfer function of input layer to hidden layer was 'tansig' (tangent sigmoid function $\tan\text{sig}(x) = \left(\dfrac{2}{1 + e^{-2x}} - 1\right)$: x is the summation of the weighted input values to the processing node) and hidden layer to output layer was 'purelin' (linear transfer function); the training function was Levenberg Marquardt (LM) algorithm (trainlm) [26]; the index of error was set as $5.98\,e^{-04}$.

We selected 4 groups of data from experimental samples as training samples to train the BP neural network. In addition, we selected the remaining data as test samples to analyze the degree of fitting between the measured values and the predicted values of neural network model.

Single neural network with four different combination of network parameters (connection weights "W" and biases

"b") was used to calculate and predict the rapidity distribution $\left(\frac{1}{N}\frac{dN}{dY}\right)$ for positive and negative poins for $\overline{p}-Au, \overline{p}-Ag$ and $\overline{p}-Mg$ interactions at P_{Lab} =100 GeV [17], the rapidity distribution of created (total charged, positive and negative) pions for $\overline{p}-Ar, \overline{p}-Xe$ collisions at P_{Lab} = 200 GeV/c [18-20] and the rapidity distribution of total charged particles for $p-Pb$ collision at $\sqrt{s}=5.02$ TeV [21]. Four different experimental data for the different interactions were used in the training phase to develop the GA-BPNN model. The training data (experimental data) were used to construct the ANN configuration and to determine the connection weights "W" and biases "b" based on the GA algorithm. The testing data were used for testing the generalization capability of the model. Therefore, four different combinations of network connection parameters (weights and biases) were used in the training phase. Connection weights, and biases for the final model are given in (Appendix A).

RESULTS AND DISCUSSIONS

To illustrate the performance of genetic algorithm for designing and optimizing the model parameters (weights and the threshold) of neural networks, this work used the same sample data. That is, we randomly selected 4 groups of data as the training sample and the rest was selected as test data to observe the training and testing performance of rapidity distribution for (h-A) collisions at P_{Lab}= 100, 200 GeV/c, $\sqrt{s}=5.02$ TeV by the GA-BPNN.

The proposed GA-BPNN model of the ($\overline{p}-Au, \overline{p}-Ag$ and $\overline{p}-Mg$) collision at P_{Lab} =100 GeV/c, $\overline{p}-Ar$, $\overline{p}-Xe$ at P_{Lab} = 200 GeV/c and $p-Pb$ collisions at $\sqrt{s}=5.02$ TeV has three inputs and one output. The inputs are: the lab momentum (P_{Lab}), the CMS rapidity (Y) of negative, positive, charged pions and the mass number (A) while the output is the rapidity distribution of negative, positive and charged pions $\left(\frac{1}{N}\frac{dN}{dY}\right)$. The ANN model is simply shown as a block diagram in Fig. 1.
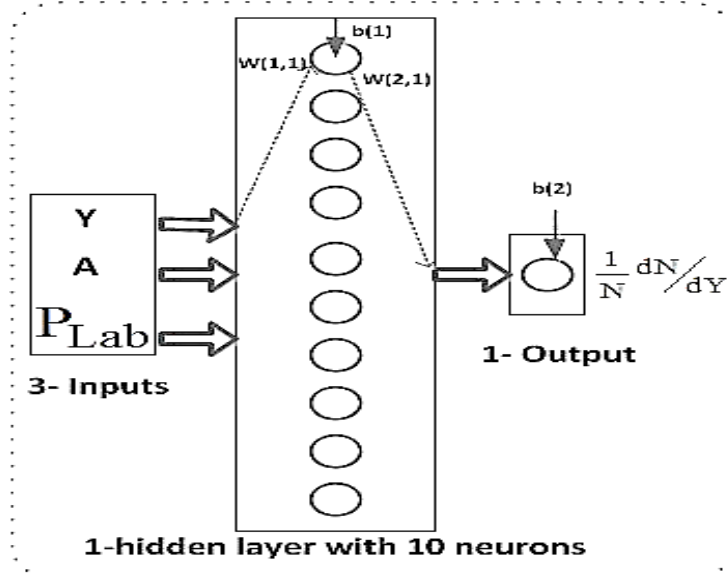
Fig.1. A block diagram of the ANN based modeling.

Using this input – output arrangement, the optimal network with four different connection parameter configurations (weights and biases) were tried to achieve good mean sum squared error (MSE) and good performance for the positive and negative pions for $\overline{p}-Au, \overline{p}-Ag$ and $\overline{p}-Mg$ interactions at P_{Lab} =100 GeV [17] the rapidity distribution of created (total charged, positive and negative) pions for $\overline{p}-Ar, \overline{p}-Xe$ collisions at P_{Lab}= 200 GeV/c [18-20] and the rapidity distribution of total charged particles for $p-Pb$ collision at $\sqrt{s}=5.02$ TeV [21].

The first configuration is dedicated for studying the negative pions of rapidity distribution $\left(\frac{1}{N}\frac{dN}{dY}\right)$ for $\overline{p}-Au, \overline{p}-Ag$ and $\overline{p}-Mg$ collisions at P_{Lab} =100 GeV/c and $\overline{p}-Ar$, $\overline{p}-Xe$ collisions at P_{Lab} =200 GeV/c. Also, one hidden layer of 10 neurons and the output layer consisting of one neuron (see Fig. 1).

The second configuration is used to simulate $\left(\frac{1}{N}\frac{dN}{dY}\right)$ for the same interactions but for the positive pions.

The third and fourth configurations of ANN, are used for charged particles resulting from $\overline{p}-Ar$, $\overline{p}-Xe$ collisions at P_{Lab} =200 GeV/c and $p-Pb$ collisions at $\sqrt{s}=5.02$ TeV respectively.

The transfer functions of the hidden layers were chosen to be a tan sigmoid for the all networks, while the output layer was chosen to be a pure line. The trained algorithm which used to train the ANN model (for the four interactions) is LM optimization technique, with number of epochs=2000.

The performance of order 10^{-4} (MSE) for the developed neural network (three inputs – one hidden layer with ten neurons and one output) at the different four configurations was around 0.0002. (See Fig. 2(a-d). The GA parameters were: populations size: 70 mutation rate: 0.01, cross-over rate: 0.1 and fitness function: MSE).
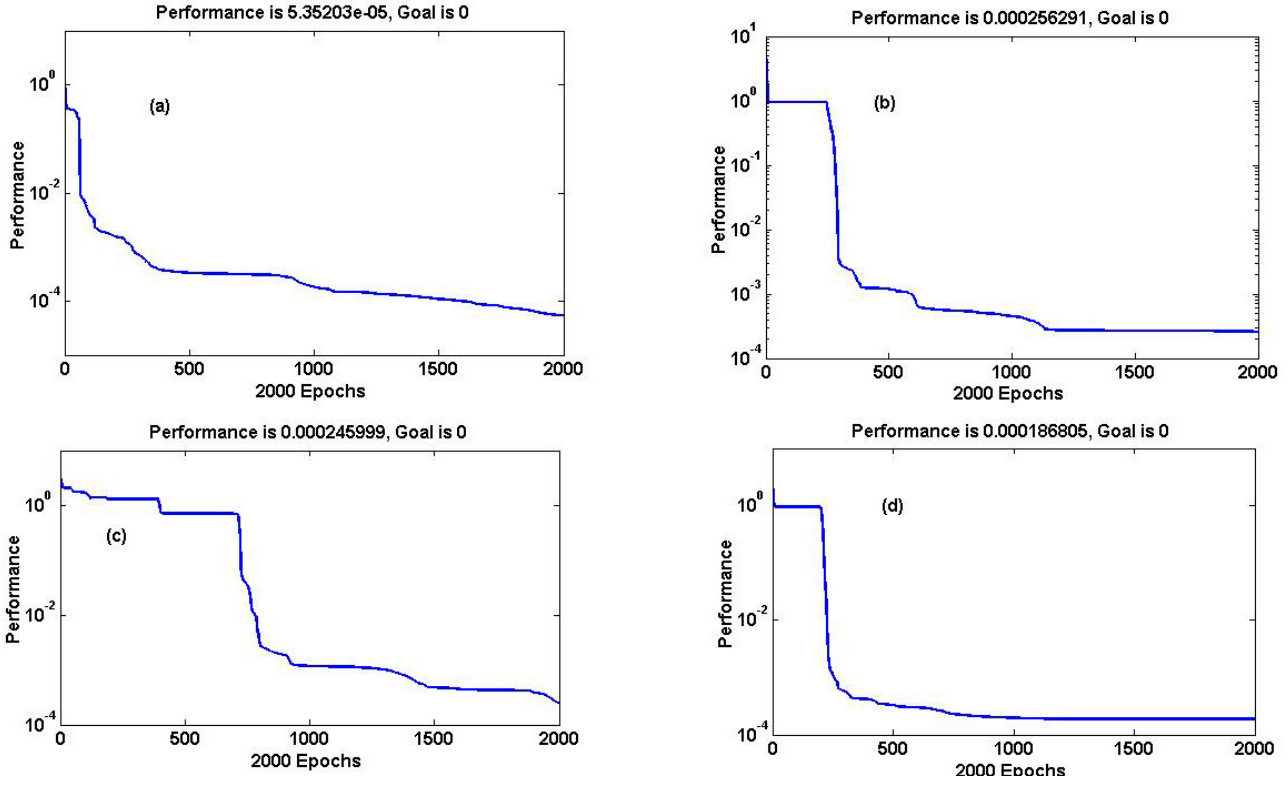
Fig. 2. The performance of the developed GA-BPNN model for (h-A) interactions
a) negative pions (P_{Lab} = 100 and 200 GeV/c), b) positive pions (P_{Lab} = 100 and 200 GeV/c), c) charged pions (P_{Lab} = 200 GeV/c) and
d) charged particles $\sqrt{s}$ = 5.02 TeV

The obtained equation (is not an explicit function in the inputs and the output) which describes the four interactions is given by:

$$\frac{1}{N}\frac{dN}{dY} = pureline \ [\{net.LW\,(2,1).\tan\ sigmoid \ .$$

$$\{net.IW\,(1,1).P + net.b\,(1)\} \ + net.b\,(2)\}] \ , \tag{8}$$

where, P: is the input which consists of three parameters, the number of particles per unit solid angle (Y), lab momentum (P_{Lab}) (or center-of-mass energy $\left(\sqrt{s}\right)$) and mass number (A).

pure line: is a linear transfer function and tan sigmoid is a hyperbolic tangent sigmoid transfer function (both of them are mathematical MATLAB transfer functions).
net. IW{1,1}: linked weights between the input layer and hidden layer.
net. LW{2,1}: linked weights between the two hidden layers.
net.b{1}   : is the bias of the first hidden layer.
net.b{2}   : is the bias of the second hidden layer.

Rapidity distribution of negative, positive and charged pions produced from $\overline{p}$ - Au, $\overline{p}$ - Ag and $\overline{p}$ - Mg collisions at P_{Lab} =100 GeV/c, $\overline{p}-Ar$, $\overline{p}-Xe$ collisions at P_{Lab} =200 GeV/c and $p-Pb$ collisions at $\sqrt{s}$ = 5.02 TeV have been simulated using Eq. (8) and compared with the corresponding experimental data.

Results of the h-A based GA-BPNN, showed in Figs. (3a,b,c,d and e (for prediction)) and in Figs. 4a,b,c,d and e (for prediction)), (5a,b) and Fig. 6 give an almost exact fitting with the experimental data. This gives the GA-BPNN the provision of a wide usage in modeling of high energy physics.
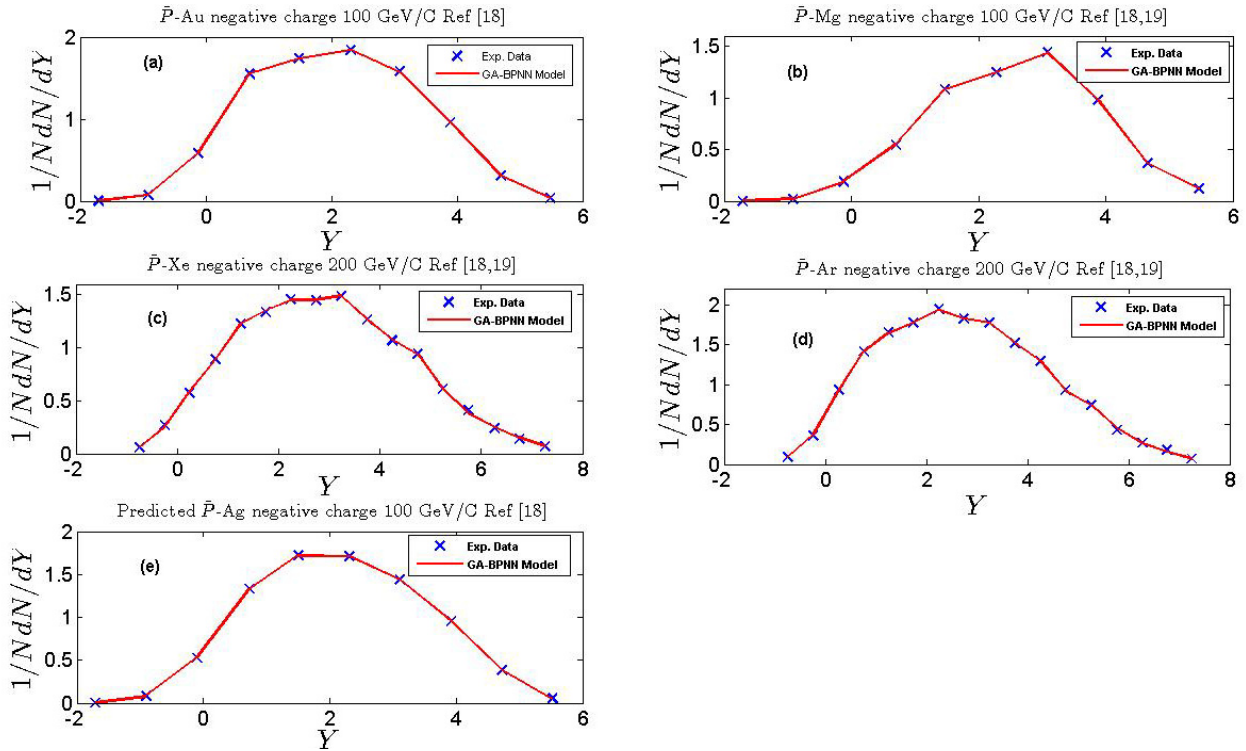
Fig. 3. Simulation of the rapidity distribution $\left(\frac{1}{N}\frac{dN}{dY}\right)$ of negative pions

a) $\bar{p}-Au$, b) $\bar{p}-Mg$ at P_{Lab} =100 GeV/c, c) $\bar{p}-Xe$, d) $\bar{p}-Ar$ at P_{Lab} =200 GeV/c using GA-BPNN model, e) Prediction of negative pions for $\bar{p}-Ag$ at P_{Lab} =100 GeV/c using GA-BPNN model (X) experimental data taken from Refs. [18, 19], (—) GA-BPNN model.
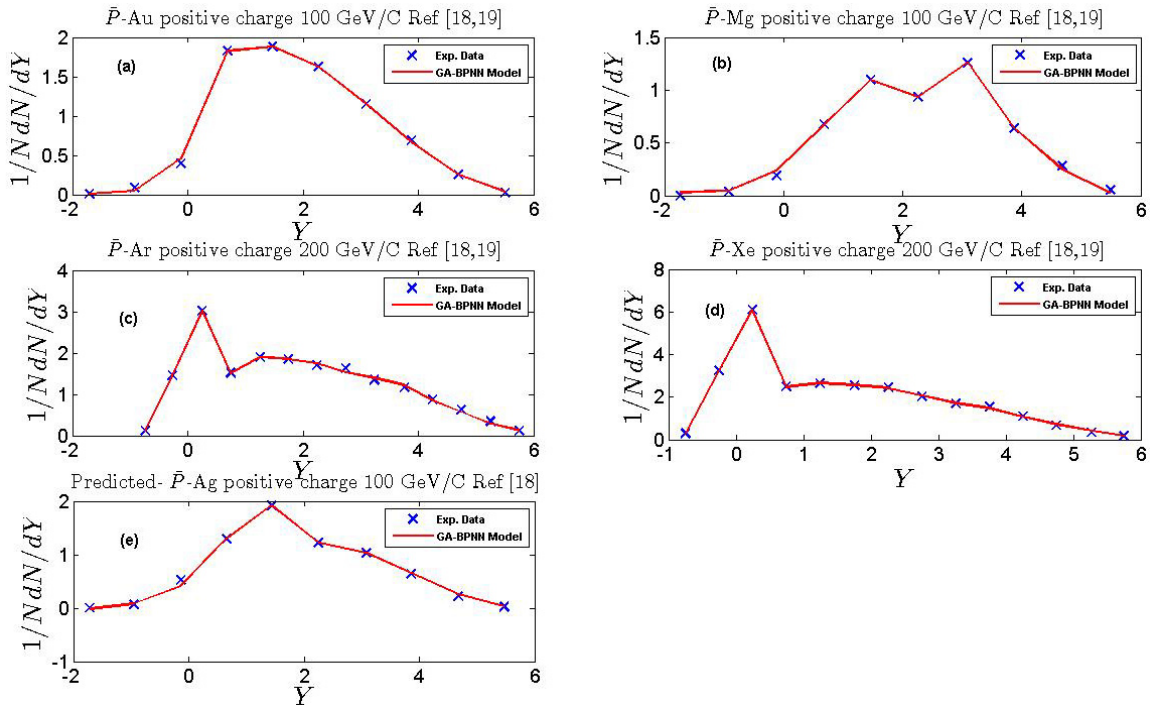
Fig. 4. Simulation of the rapidity distribution $\left(\frac{1}{N}\frac{dN}{dY}\right)$ of positive pions

a) $\bar{p}-Au$, b) $\bar{p}-Mg$ at P_{Lab} = 100 GeV/c, c) $\bar{p}-Ar$, d) $\bar{p}-Xe$ at P_{Lab} =200 GeV/c using GA-BPNN model, e) Prediction of positive pions for $\bar{p}-Ag$ at P_{Lab} =100 GeV/c using GA-BPNN model, (X) experimental data taken from Ref. [18-19], (—) GA-BPNN model.

GA-BPNN model has been shown to be a useful method for modeling the h-A interactions. All the figures showed a clear and excellent match to the experimental data [17-21].

Also, from these figures we can see that the proposed GA-BPNN model in this paper can describe and predict effectively sub nuclear interactions at high and ultrahigh energies.
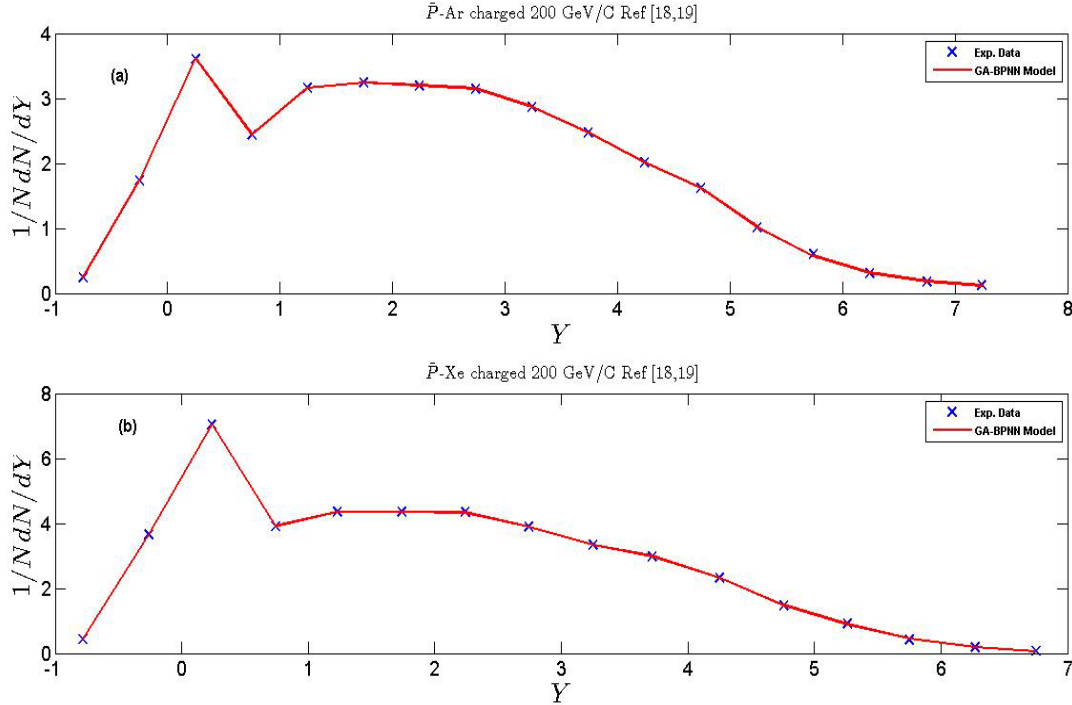
Fig. 5. Simulation of the rapidity distribution $\left(\frac{1}{N}\frac{dN}{dY}\right)$ of charged pions

a) $\bar{p} - Ar$, b) $\bar{p} - Xe$ at P_{Lab} = 200 GeV/c using GA-BPNN model,(X) experimental data taken from Refs. [18, 19], (—) GA-BPNN model.
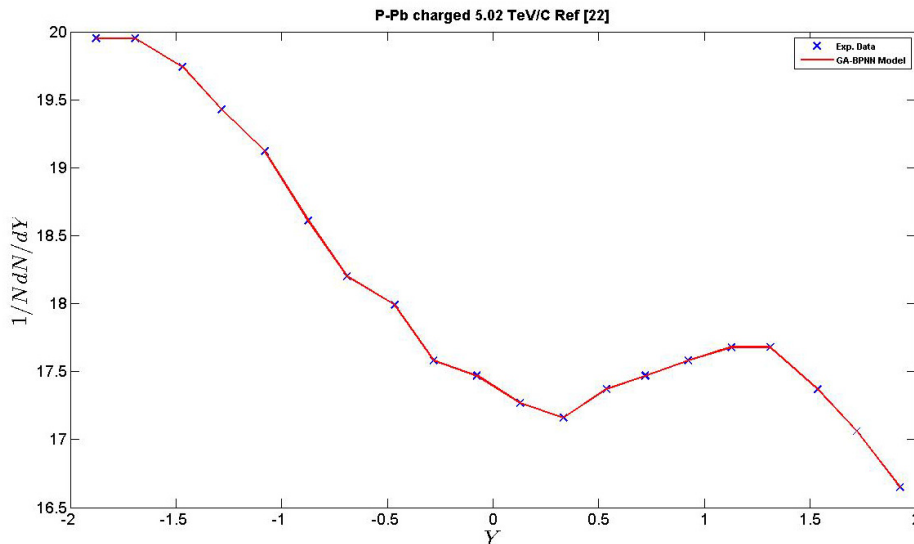
Fig. 6. Simulation of the rapidity distribution $\left(\frac{1}{N}\frac{dN}{dY}\right)$ of charged particles for $p - Pb$ at $\sqrt{s}$ =5.02 TeV using GA-BPNN model,

(X) experimental data taken from Ref. [22], (—) GA-BPNN model.

CONCLUSIONS

The traditional mathematical models that studied the rapidity distribution $\left(\frac{1}{N}\frac{dN}{dY}\right)$ have some defects in different

degrees, which cannot accurately explain the phenomenon of multiparticle production mechanism. This paper introduced two intelligent algorithms by consulting relevant references, such as neural network and genetic algorithm,

to build the GA-BPNN model of rapidity distribution and implement relevant optimization. The rapidity distribution of negative, positive and charged pions for $\overline{p} - Au, \overline{p} - Ag$ and $\overline{p} - Mg$ interactions at $P_{Lab} = 100$ GeV/c and for $\overline{p} - Ar$, $\overline{p} - Xe$ interactions at $P_{Lab} = 200$ GeV/c and $p - Pb$ collisions at $\sqrt{s} = 5.02$ TeV have been simulated using Eq.(8) and compared with the corresponding experimental data. Finally, we conclude that GA-BPNN model can be used as a suitable approach in predicting selected observables of high and ultrahigh energy physics interactions.

REFERENCES

1. Tantawy M., El-Mashad M., El-Bakry M.Y. Multiparticle Production Process in High Energy Nucleus-Nucleus Collisions // Ind. J. Phys. – 1998. –Vol. 72A. – No.1. – P.73-82.
2. Tantawy M., El Mashad M., Gamiel S., El Nagdy M.S. Multiplicity distribution of heavy particles for hadron–nucleus interactions // Chaos Soliton Fract. – 2002. – Vo1.3. – No.4. – P.919–928.
3. Ranft J. Secondary particle production according to the thermodynamical model and new experimental data // Phys. Lett. B. – 1970. – Vol.31. – No.8. – P.529-532.
4. Fermi E. High Energy Nuclear Events // Prog. Theor. Phys. – 1950. – Vol.5. – No.4. – P.570 -583.
5. Fermi E. Angular Distribution of the Pions Produced in High Energy Nuclear Collisions // Phys. Rev. – 1951. – Vol 81. – No.5. – P.683-687.
6. Jacob M., Slansky R. Inclusive pion distributions at present machine energy // Phys. Lett. B. – 1971. – Vol. 37. – No.4. - P. 408-412.
7. Hwa R.C. Multiplicity Distribution and Single-Particle Spectrum in the Diffractive Model // Phys. Rev. Lett.. – 1971. – Vol.26. – No.18. – P.1143.
8. Hwa R.C. Bootstrap Model for Diffractive Processes: Complementarity of the Yang and Regge Models // Phys. Rev. D. - 1970. – Vol.1. – No.6. – P.1790.
9. Kisslinger L.S. Nuclear physics and quark/gluon QCD // Nucl. Phys. A. – 1985. – Vol.446. – No.1. – P.479-488.
10. Gyulassy M. Introduction to QCD thermodynamics and the quark-gluon plasma // Progress in Particle and Nuclear Physics. - 1985. – Vol.15. – P.403-442.
11. Nambu Y. The confinement of quarks // Sci Am. – 1976. – Vol.235. – No.45. – P. 48-61.
12. Xu, C., Wei-Qin, C., Ta-Chung, M., Chao-Shang, H. (1986). Statistical approach to nondiffractive hadron-hadron collisions: Multiplicity distributions and correlations in different rapidity intervals // Phys. Rev. D. – Vol.33. – No.5. – P. 1287.
13. El-Bakry S.Y., El-Dahshan E.S., El-Bakry M.Y. Total cross section prediction of the collisions of positrons and electrons with alkali atoms using Gradient Tree Boosting // Ind. J. Phys. 2011. – Vol. 85. – No.9. – P.1405-1415.
14. El-Bakry M.Y. Feed forward neural networks modeling for K–P interactions // Chaos Soliton Fract. – 2003. – Vol. 18. – No.5. –P. 995-1000.
15. El-Dahshan, E., Radi, A., El-Bakry M.Y. Artificial Neural Network and Genetic Algorithm Hybrid Technique for Nucleus-Neuclus Collisions // Int. J. of Mod. Phys. C. – 2008. – Vol.19. – No.12. – P.1787-1795.
16. El-Bakry M.Y., El-Dahshan E.S.A., El-Bakry S.Y. Mathematical modelling for pseudorapidity distribution of hadron-hadron collisions // Eur. Phys. J. Plus. – 2015. – Vol.130. – No.1. – P.1-7.
17. El-Bakry M.Y., El-Dahshan E.S.A., Radi A. ,Tantawy M., Moussa M.A. Modeling and Simulation for High Energy Sub-Nuclear Interactions Using Evolutionary Computation Technique // Journal of Applied Mathematics and Physic – 2016. - Vol.4. – No.1. – P. 53-65.
18. Whitmore J.J., Persi F., Toothacker W.S., Elcombe P.A., Hill J.C., Neale W.W., Ammar R. Inclusive charged pion production in hadron-nucleus interactions at 100 and 320 GeV/c // Z. Phys. C Part Field. – 1994. – Vol.62. – No.2. – P. 199-227.
19. De Marzo C., De Palma M., Distante A., Favuzzi C., Germinario G., Lavopa P. & Spinelli P. Multiparticle production on hydrogen, argon, and xenon targets in a streamer chamber by 200-GeV/c proton and antiproton beams // Phys. Rev. D. – 1982. – Vol.26. – No.5. – P.1019.
20. Arneodo M., Arvidson A., Aubert J.J., Badełek B., Beaufays J., Bee C.P., Böhm, E. Comparison of multiplicity distributions to the negative binomial distribution in muon-proton scattering // Z. Phys. C. Part Field. – 1987. – Vol.35. – No.3. – P.335-345.
21. Kittel W. Combining inclusive and exclusive data analyses-what have we learned so far? //J. Phys A-Math. Gen. – 1973. – Vol.6. – No.6. – P.733.
22. Abelev B., Adam J., Adamová D., Adare A.M., Aggarwal M.M., Rinella G.A., Ahmad N. Pseudorapidity density of charged particles in p+ Pb collisions at $\sqrt{S_{NN}} = 5.02$ TeV // Phys. Rev. lett. – 2013. – Vol.110. – No.3. – P.032301.
23. Guettler K., Duff, B.G., Prentice M.N., Sharrock S.J., Gibson W.M., Duane A., Henning S. Inclusive production of low-momentum charged pions at x= 0 at the CERN intersecting storage rings // Phys. Lett. B. – 1976. – Vol. 64. – No.1. – P.111-116.
24. Adamovich M.I., Chernjavskii M.M., Dremin I.M., Gershkovich A.M., Kharlamov S.P., Larionova V.G., Yagudina F.R. Clusters and the rapidity interval method. Il Nuovo Cimento A. – 1976. – Vol.33. – No.1. – P.183-194
25. Haykin S.S., et al. Neural networks and learning machines. – 2009. – Vol.3. Upper Saddle River: Pearson Education.
26. Chipperfield A.J., Fleming P.J. The MATLAB genetic algorithm toolbox / Applied control techniques using MATLAB, IEE Colloquium on. – 1995, January. – P.10/1-10/4.

Appendix A

Configurations of connection parameters (weights and biases) for the rapidity distribution of negative, positive and charged pions for $\bar{p} - Au, \bar{p} - Ag$ and $\bar{p} - Mg$ interactions at P_{Lab} =100 GeV/c and for $\bar{p} - Ar, \bar{p} - Xe$ interactions at P_{Lab} = 200 GeV/c and $p - Pb$ collisions at $\sqrt{s}$ =5.02 TeV:

I-Negative pions at 100 and 200 GeV/c												
W(1,1)			**W(2,1)**									
-0.54482	0.332892	-0.25255	0.711	0.26273	0.56918	0.575748	0.23744	0.015845	0.6588	0.801588	0.34678	0.57328
0.633076	0.52869	-0.53915										
1	-0.00847	0.140593										
0.041907	-0.25837	-0.28255										
-0.03047	-0.30283	-0.26994										
-0.47298	0.057861	-0.49468										
-0.14539	-0.43576	0.840097										
-0.33804	-0.30108	0.010292										
0.67309	-0.44042	0.085003										
0.366667	-0.22427	0.732896										
b(1)			**b(2)** 0.832897									
-0.36364												
0.523865												
1												
-0.8229												
0.713279												
0.442266												
-0.19545												
0.192635												
-0.46723												
-0.19355												

II-Positive pions at 100 and 200 GeV/c												
W(1,1)			**W(2,1)**									
-0.50692	-0.61571	0.156851	0.233132	0.054168	0.76479	0.869325	0.880007	0.540102	0.01847	-0.2292	0.15661	1
-0.72344	0.87674	-0.16989										
0.125749	-0.48477	-0.68577										
-0.81411	-0.73901	-0.03509										
0.900245	-0.49287	-0.89428										
-0.9861	0.84631	0.174089										
0.135711	-0.75487	0.976662										
-0.52165	0.471073	-0.66146										
-0.78399	-0.17519	0.858352										
0.68431	-0.43682	0.800259										
b(1)			**b(2)** -0.00717									
-0.80006												
-0.48338												
0.565427												
0.268225												
0.54297												
-0.53119												
-0.5458												
0.68937												
0.320663												
0.349154												

III-Charged pions at 200 GeV/c.												
W(1,1)			**W(2,1)**									
0.615044	0.630483	-1	0.221102	0.178165	0.160589	0.54989	0.81778	0.45187	0.51432	0.18236	0.158732	0.884721
0.574515	-0.24201	0.96063										
0.336177	0.194511	-0.60853										
0.702738	-0.2709	0.544958										
-0.71844	0.026173	-0.42179										
-1	-0.63519	-0.60805										
0.001897	-0.4758	-0.87851										
0.202478	0.061921	-0.32841										
0.924715	0.041567	-0.69068										
0.33577	-0.07237	-0.99096										
b(1)			**b(2)**									
-0.02228			-0.20985									
0.544593												
0.987502												
-0.78824												
0.310195												
-0.74454												
-1												
-0.85451												
0.403024												
0.6188												

IV-Charged particles at 5.02 TeV.												
W(1,1)			**W(2,1)**									
-0.71416	-0.92088	0.325213	0.958607	0.93462	0.26646	0.752368	0.69604	0.652702	0.945123	0.106815	0.724473	0.198673
0.445217	0.081723	-0.03832										
0.395764	0.446531	0.926526										
-0.45433	0.118438	-0.29796										
-1	0.594756	-0.3562										
0.222468	0.05708	-0.44014										
0.164204	0.266714	-0.15557										
-0.55492	-0.37292	0.236666										
0.900786	0.073083	-1										
-0.28479	-0.76652	-0.16525										
b(1)			**b(2)**									
0.379108			-0.32899									
0.971519												
-0.93134												
-0.57285												
0.236435												
0.096667												
-0.90753												
0.553708												
-0.80058												
0.153643												